

RENEWABLE SOURCES URBAN CELLS MICROGRID: A CASE STUDY

S. AGOSTINELLI, F. NARDECCHIA & L. POMPEI

Department of Astronautics, Electrical and Energy Engineering, Sapienza University of Rome, Italy.

ABSTRACT

Nowadays, microgrid technologies play a relevant role in the research field as well as in the commercial market. The opportunity to provide electricity in wide areas without using centralized electrical infrastructure networks is a reliable key for achieving the European Union sustainability goals. In this regard, the proposed research aims at describing an electric microgrid configuration powered by a photovoltaic system, supplying three school buildings located in the center of Italy. Additionally, the resilience theme is deeply investigated, analyzing the use of an emergency generator system (EGS) in case of electric grid blackouts. MATLAB/Simulink was chosen to simulate the users' energy demand as well as to calculate the microgrid performance. Results show that almost the total consumption of the microgrid is covered by the photovoltaic system, and the use of an EGS allows energy resilience and moderate economic savings for the community.

Keywords: Backup diesel generators, community resilience, microgrid, photovoltaic solar energy, renewable sources, school buildings.

1 INTRODUCTION

The use of energy systems based on microgrid technology is assuming a relevant role in the research field as well as in the commercial market, due to their application in urban settlements. The inclusion of microgrid technologies into real-world applications depends on the evolution of the electricity systems based on 'decentralizing, decarbonizing, and democratizing' concepts. Those three 'Ds' are focused on the reduction of fossil fuel emissions, as well as on the improvement of resilience in urban contexts [1]. Integrating renewable energy sources (RES) is another relevant objective, following the current European directives [2]. The flexibility of microgrid systems lead the national government and policies to adapt it into different frameworks, from industrial areas to rural lands, where inhabitants could frequently face unaffordable electricity services [3]. Therefore, microgrids are not a rigid energy system infrastructure, but their configuration depends on project's requirements, geographical location, and economic evaluations [1]. The type of energy generation source is included in a wide range, from diesel combustion engines and micro turbine, fuel cells to renewable generation [4–6]. The energy storage system is not strictly required, but it is commonly used to guarantee the electricity supply [7].

Furthermore, a consistent advantage of microgrid systems is energy resilience, which has been widely investigated in the last years, showing the importance to increase its power for energy systems. In detail, four aspects are involved in developing an electrical system into a resilience one: failure prevention, energy and economic consequences mitigation, reduction of time response, and recovery of the electricity supply [8]. To face

blackout's events, backup diesel generators (BDGs) are used, combined with energy storage where necessary [9]. Moreover, the energy resilience concept is fundamental for the evolution of Smart Cities: in fact, a Smart City is expected to have minimal environmental impacts, regulated electricity consumptions, and environmentally responsible citizens. The future of Smart Cities is linked to energy resilience as, the more a urban center is able to cope with environmental changes, the more it will be able to provide positive reactions [10].

As mentioned earlier, the current work is focused on the role of the RES in reducing CO₂ emissions, electricity costs, and energy consumption through the development of a microgrid for an Italian urban context. The BDGs is involved to ensure the resilience of the system [9].

Many works in literature propose different microgrid configurations, investigating the design and simulation of a hybrid microgrid to test its efficiency and reliability [11]; focusing on the relation between microgrid and Near Zero Energy Buildings (nZEBs) assessments, according to the optimization of the model [12, 13]. On the other hand, researchers [14] analyze smart grids, highlighting its importance to reduce the peak of energy demand. Finally, Rosales-Asensio *et al.* [15] investigate the opportunity to develop a microgrid supplying a large office building, providing advantages in terms of economic savings and resilience performance. Moreover, in this study, the use of photovoltaic panels as the RES supplying a microgrid system presents several advantages, being the most common RES technology for this purpose [1, 15]. Office buildings, rural lands, military site, and public complex are investigated as case studies in different works [1, 11, 15]. Instead, the microgrid presented by the authors is connected to three school buildings, located in Terracina, a small city in the center of Italy. The entire model is simulated using MATLAB/Simulink, allowing the definition of the geometrical configuration and energy balance of the case study. The combination of the photovoltaic solar energy and a BDG shows the reliability of the presented microgrid, even in case of failure events. Particularly, results show how the photovoltaic panel production covers the entire consumption of the microgrid in good weather conditions. Furthermore, during the warmer months, an excess of electricity production is available allowing to extend the system to different users. Only a limited amount of energy comes from the national grid. In case of a national grid failure, a 250-kW methane emergency generator (EG) was set up ensuring the system resilience. The results of the analysis highlight the use of an emergency generator system (EGS) allowing a good resilience of urban energy systems and some economic savings for communities.

2 CASE STUDY DESCRIPTION

Terracina is an Italian town of 43,639 inhabitants located in the province of Latina. The city is placed in the Agro Pontino at the southern edge of the plain, at south of the promontory of Circeo, near to the mouth of the river Amaseno, on the Tyrrhenian coast (gulf of Gaeta); the city is an appendix of the Monte Sant'Angelo, where the historical center is located, up to the promenade Circe. The cliff of Pisco Montano clearly marks the southern boundary of the town; southwards the plain of Fondi opens, northwards the urbanization progressively decreases towards the open country and the rural villages. Terracina, historically the main attraction of the Latium Riviera, focuses its economy on tourism and services sector. Its transformation into a smart city would allow it to maintain its leading role in this sector by offering better, innovative, and more efficient services to tourists and citizens, while boosting the city's economy.

2.1 Building 1

The first considered building hosts a school for a total of about 1,000 students. The total area occupied by the building complex is approximately 14,000 m² (Fig. 1).

The school complex consists of two buildings: the larger one has two floors with a total area of 6,726 m² and the smaller one has three floors with a total area of 2,070 m²; building dimensions are shown in Table 1.

The heating system consists of 105 two-pipe fan-coils, each with a maximum flow rate of 231 m/h. The system is able to achieve the internal environment set point temperature, and once the maximum limit is reached, it reduces its flow rate to 30%, as to maintain optimal



Figure 1. Building 1.

Table 1: Building 1 dimensions.

Building 1 dimensions	
Type floor area	3,363 m ²
Floors number	2
Storey height	3.2 m
Total gross area	6,726 m ²
Wall thickness	0.4 m
Total net area	6,527.48 m ²
Windows area	265 m ²
Volume	21,523.2 m ³

internal conditions and avoid excessive stress on the terminal, due to on–off operations. If the reduction of the flow rate would not allow to keep the internal temperature above the minimum limit, the system returns to nominal flow rate operation. Specifically, Terracina (climate zone D), requires the start-up period to be between 1 November and 15 April, keeping the internal temperature at $20\text{ }^{\circ}\text{C} \pm 2\text{ }^{\circ}\text{C}$.

The lighting system consists of about 600 tubular neon lamps of 36 W each, obtaining 300 lux in classrooms, according to UNI EN 12464-1 [16].

The Simulink diagram in Fig. 2 aims to monitor the operation of the heating system and the temperature trend in the Building 1.

In order to study the temperature trend inside the building, it was necessary to determine the thermal loads as follows:

- thermal dispersions towards the outside caused by the difference in temperature between the heated environment and the outside;
- dispersions due to air infiltration through the glazed surfaces;
- internal load due to the presence of people in the structure;
- internal load due to the lighting system.

Since none of the described thermal loads appears to be constant during the day, it was considered the hourly variation to develop a realistic simulation. The central heating system is switched on at 7:00 and turned off at 18:00, when the school is empty.

The electrical utilities inside the building are as follows:

- 105 fan-coils (rated power 32 W);
- 604 neon tubular lamps (nominal power 36 W);
- 191 electronic appliances (average power 100 W).

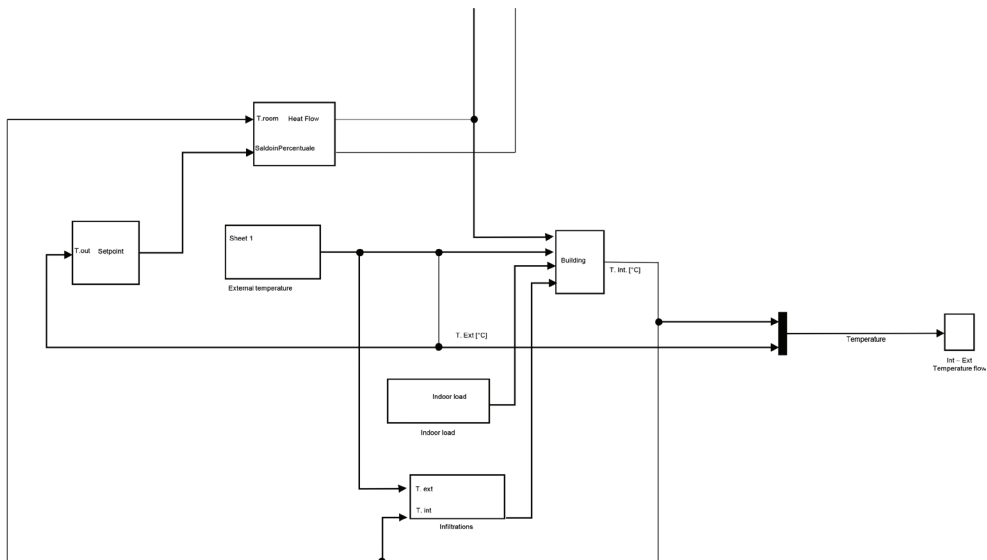


Figure 2: Building 1 Simulink diagram.

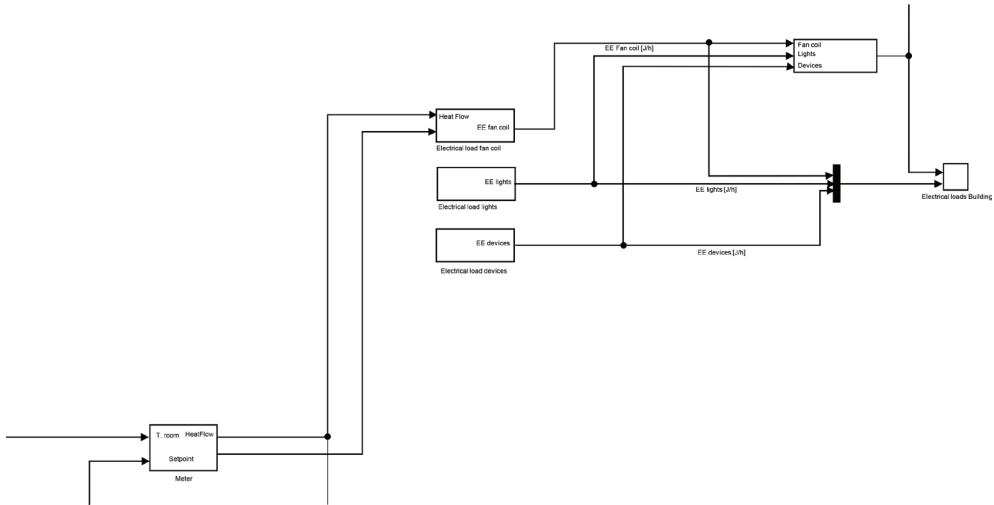


Figure 3: Simulink diagram of electrical loads - high school building.

Table 2: Building 2 dimensions.

Building 2 dimensions

Type floor area	690 m ²
Floors number	3
Storey height	3.2 m
Total gross area	2,070 m ²
Wall thickness	0.4 m
Total net area	1,942.8 m ²
Windows area	170 m ²
Volume	6,624 m ³

Figure 3 shows the Simulink block diagram for simulating the operation of electrical loads within the structure.

2.2 Building 2

The year of construction and structure data are the same as those reported for Building 1. Dimensions of the small building are shown in Table 2.

Following the same operation logic as the other building, the heating system consists of 41 two-pipe fan-coils, each with a maximum capacity of 231 m³/h. The lighting system consists of about 180 tubular neon lamps of 36 W each, obtaining 300 lux in the classrooms, as required by UNI EN 12464-1 [16]. The Simulink diagram shown in Fig. 4 aims to monitor the operation of the heating system and the temperature trend inside the small building.

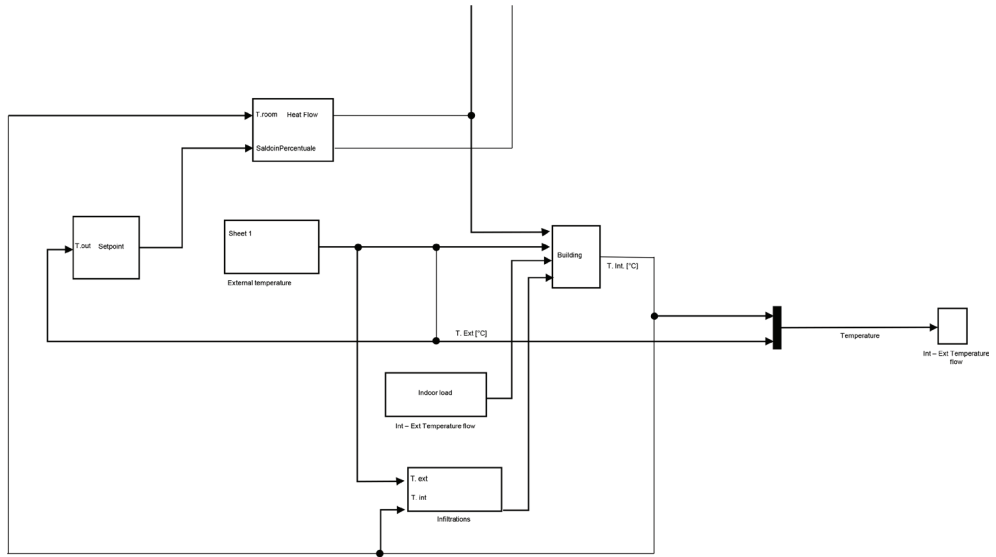


Figure 4: Building 2 Simulink diagram.

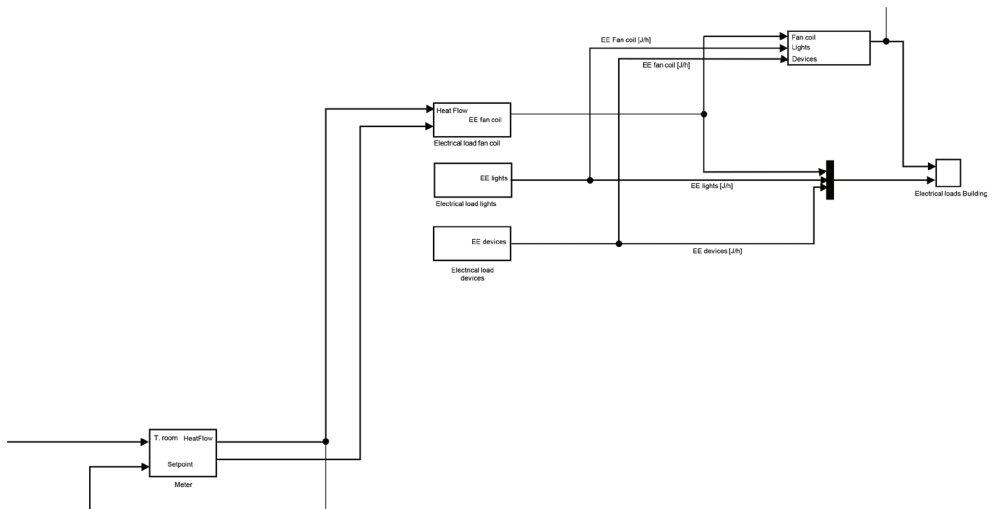


Figure 5: Simulink diagram of electrical loads – Building 2.

The electrical utilities within the building are as follows:

- 41 fan-coils (rated power 32 W);
- 180 neon tubular lamps (nominal power 36 W);
- 9 electronic appliances (average power 100 W).

Figure 5 shows the Simulink block diagram for the simulation of the operation of electrical loads within the structure.

2.3 Building 3

The institute hosts about 700 students, and the total area occupied by the building complex is about 10,000 m².

Thanks to the on-site inspections conducted in the building, information about the year of construction and data on the structure were obtained. The building was built in 1976, with reinforced concrete bearing structure and floors, while the windows are single-glazed. By consulting the technical norms of the Ministerial Decree of 18 December 1975 [17], it was possible to determine the thermal transmittance parameters of both the envelope and the windows (reported in Table 1). The dimensions of the building are reported in Table 3.

Following the same operation logic as the high school, the heating system consists of 104 two-pipe fan-coils, each with a maximum flow rate of 231 m³/h. While setting the simulation parameters, the law of 9 January 1991 was considered for determining the period of ignition of the heating system and the temperature to be maintained in the indoor environments according to the climatic zone. The Simulink scheme shown in Fig. 6 aims to monitor the operation of the heating system and the temperature trend inside the institute.

The electrical utilities within the building are as follows:

- 104 fan-coils (rated power 32 W);
- 679 neon tubular lamps (nominal power 36 W);
- 103 electronic appliances (average power 100 W).

Figure 7 shows the Simulink block diagram for simulating the operation of electrical loads within the structure.

3 MICROGRID

As mentioned earlier, nowadays resilience represents a fundamental factor for the improvement of energy efficiency, as well as for the sustainable development of a city, favoring the adoption of renewable sources for the energy production.

The two school complexes (Building 1 and Building 2) are considered critical poles of the city of Terracina, located about 200 m far from each other. These two scholastic structures

Table 3: Building 3 dimensions.

Building 3 dimensions	
Type floor area	3,775 m ²
Floors number	2
Storey height	3.2 m
Total gross area	7,550 m ²
Wall thickness	0.4 m
Total net area	7,338 m ²
Windows area	283 m ²
Volume	24,260 m ³

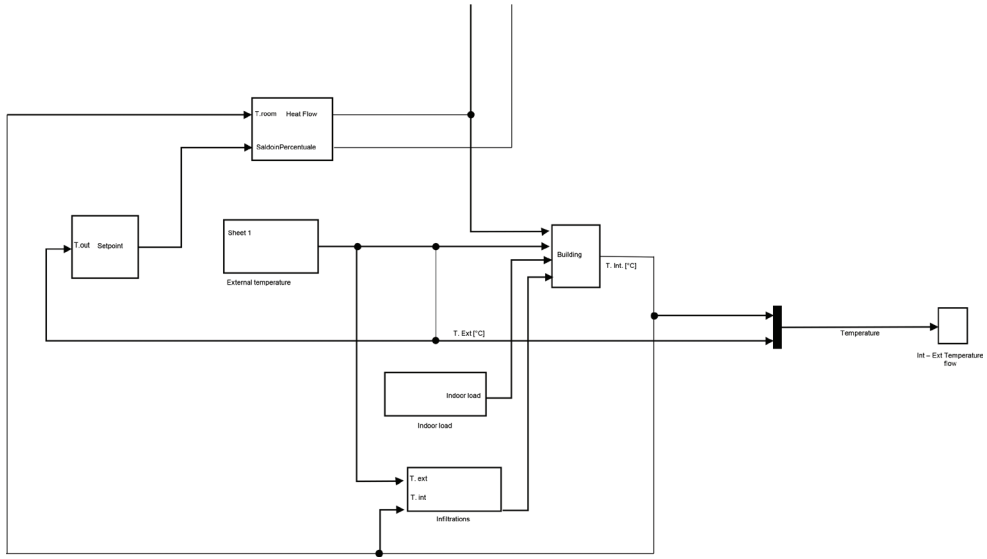


Figure 6: Building 3 Simulink diagram.

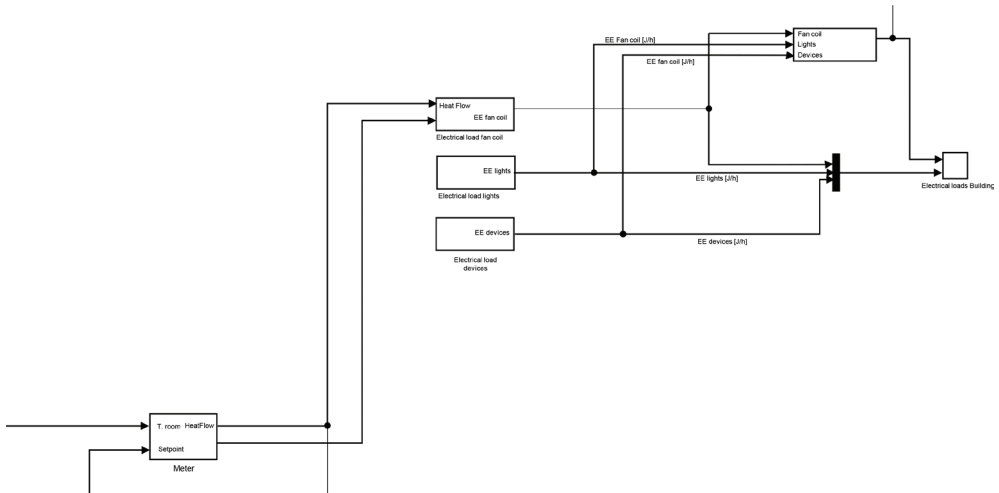


Figure 7: Simulink diagram of electrical loads – Building 3.

host almost 2,000 students, coming from the neighboring areas, since the other institutes are located at a distance of about 40 km; for this reason, it is necessary to guarantee the continuity of the scholastic activities also in case of lack of power supply from the electric network.

As considered, a microgrid system supplying the three school buildings was realized. The microgrid system supplies: Building 1; Building 2; Building 3; the photovoltaic system placed on the roof of Building 2. Therefore, these are also the electrical loads fed by the microgrid.

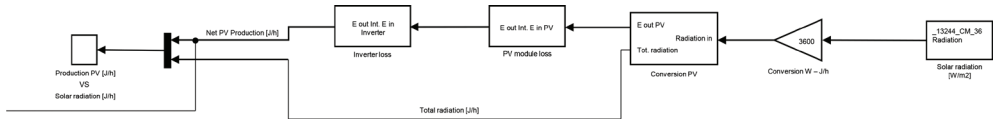


Figure 8: Simulink diagram - Generation from photovoltaic system.

Table 4: Components of the photovoltaic system.

Photovoltaic field features

Photovoltaic module

Model	SPR-X21-345
Brand	Sun Power
Number of photovoltaic modules	12 modules in series 74 strings in parallel
Total number of photovoltaic modules	888
Rated unit power	345 W _p
Overall field power rating	306 kW _p
Total area	1448 m ²

Inverter

Model	ECO 27.0-3-S
Brand	Fronius International
Operating voltage	580–850 V
Rated unit power	283 kW _{ac}
Inverter group	10 units
Total power	270 kW _{ac}

The main objective of this project is to minimize the inconvenience caused to citizens in case of blackouts, thus ensuring the normal performance of essential services such as school education. To power the proposed microgrid, a photovoltaic system has been installed on the roof of Building 2. Figure 8 shows the Simulink diagram of the photovoltaic system. Starting from the hourly solar radiation incident on the roof of the institute, and considering system losses, the net production of the photovoltaic system was calculated to 501 MWh per year.

With the help of PVsyst software [18], it was possible to correctly size the PV system to be installed and quantify the actual system losses. The characteristics of the chosen components are shown in Table 4.

4 RESULTS

In this section, the energy simulation results will be presented for the considered buildings and the hypothesized microgrid. Initially, thermal and electrical loads of the three main buildings are analyzed, then the power contribution of photovoltaic panels in the microgrid is evaluated. Then, the electrical loads and related costs to full operation as well as the presence of a random grid failure will be shown.

4.1 Building 1

The considered period for the simulation corresponds to the Italian school-year, from the beginning of September to the end of June as July; August was not considered, being no significant activities in the school. Figure 9 shows the trend of the external temperature in Terracina (blue) and the temperature inside the building (yellow) in the considered period. The operating period of the heating system is highlighted by the red arrow, and it is possible to notice how, thanks to the functioning of the heating system, the internal temperature is maintained between 18 and 22 degrees.

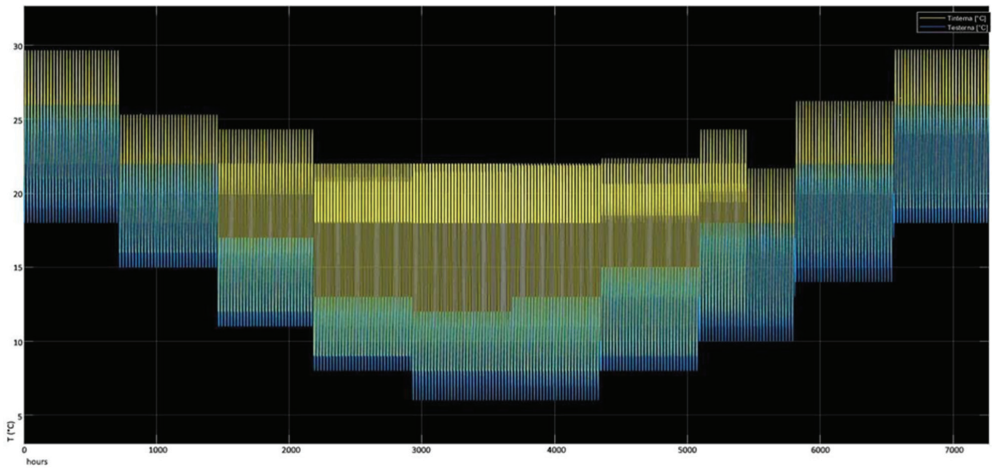


Figure 9: Global temperature trends.

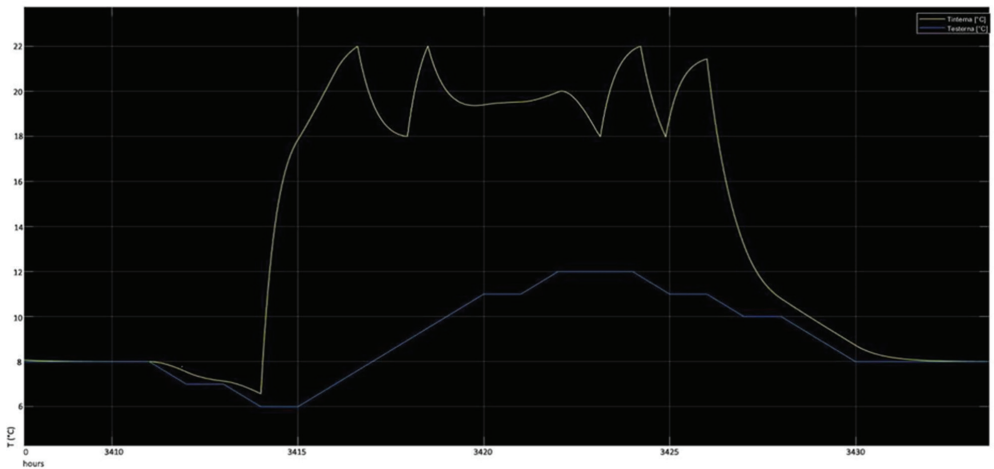


Figure 10: Daily temperature trends in January.

Analyzing in detail a typical winter day (January), it is evident how the heating system turns on at nominal flow rate until the maximum limit of 22 °C is reached, varying the flow rate in order to keep indoor comfortable conditions (Fig. 10).

In the spring period, being warm external temperatures, it can be noted that flow rate reductions to 30% for the most of the day is sufficient to keep the indoor temperature within the set limits (Fig. 11).

For the electrical part, weekly and daily load curves are shown in Figs 12 and 13. The maximum annual absorption is 44.19 kW in December. The daily load curve shows that the main electricity user is the lighting system, with an average absorption of 21.77 kW.

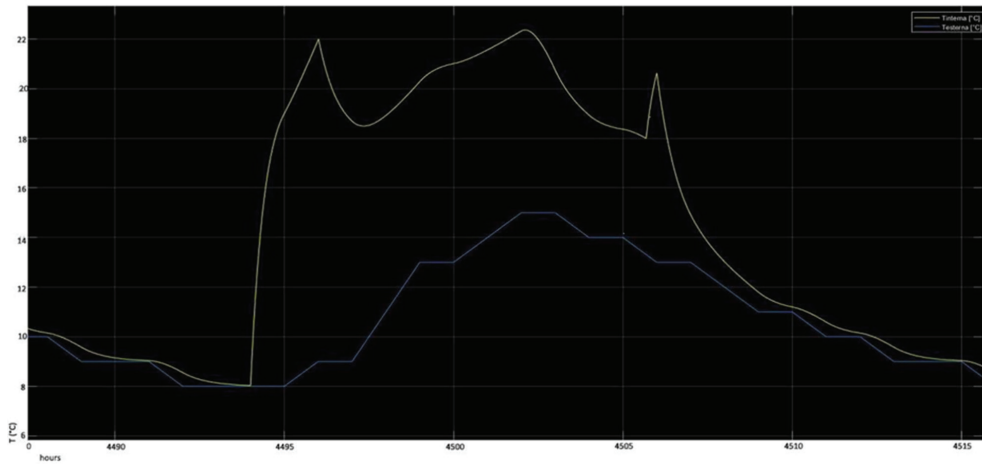


Figure 11: Daily temperature trends in March.

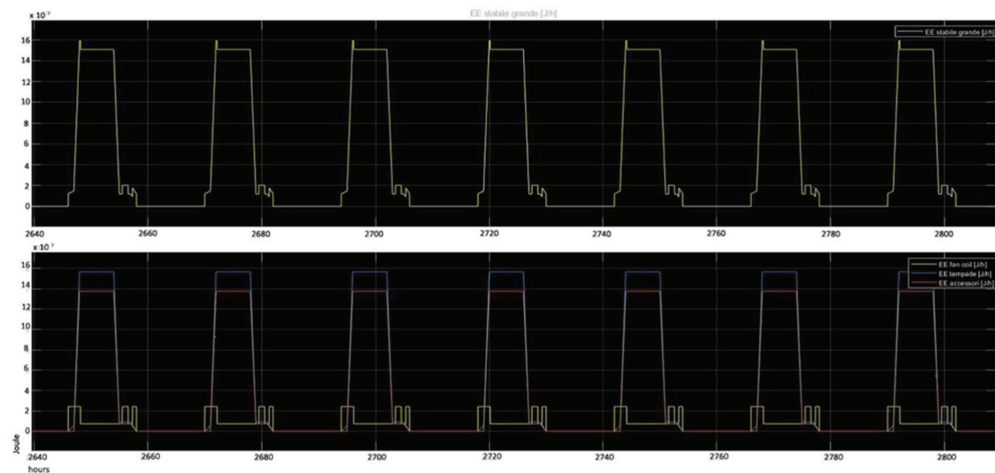


Figure 12: Weekly load curve Building 1.

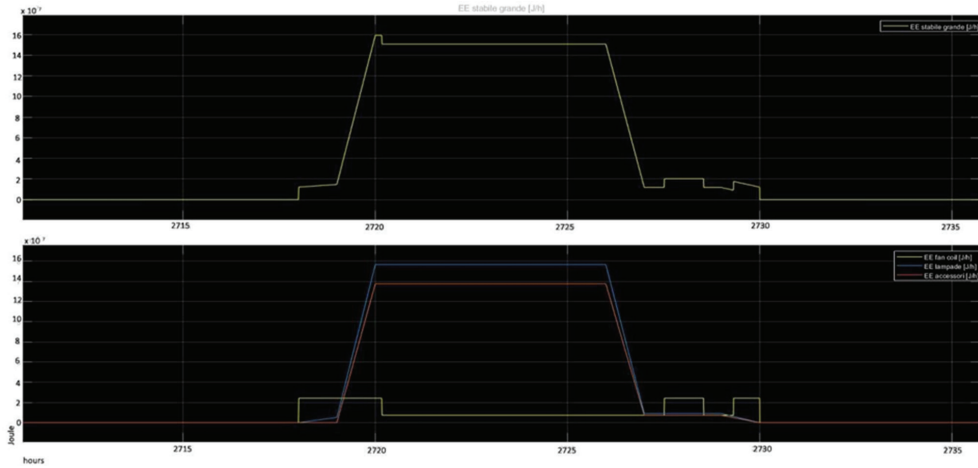


Figure 13: Daily load curve Building 1.

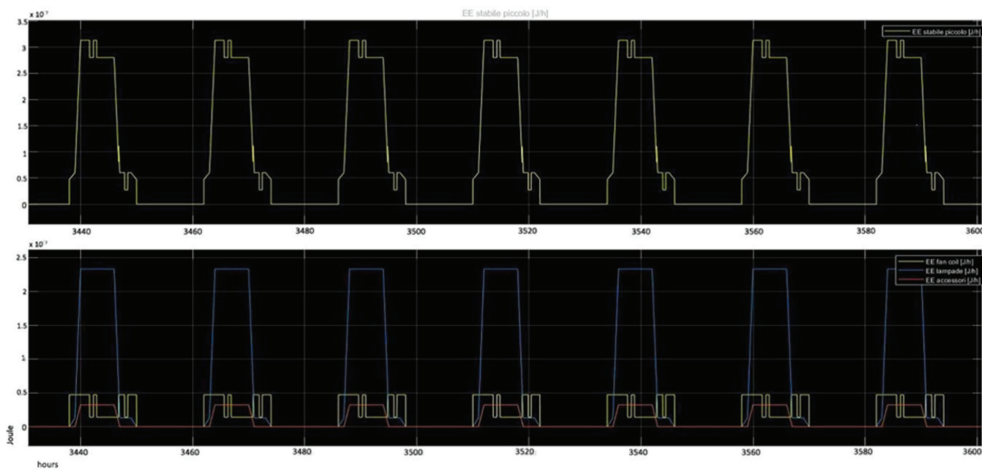


Figure 14: Building 2 weekly load curve.

4.2 Building 2

The obtained temperature results through the Building 2 simulation have the same trend as those previously reported for Building 1. The weekly and daily load curves are shown in Figs 14 and 15. The maximum annual absorption is in December and is equal to 8.7 kW. As shown by the daily load curve, the main electricity user is the lighting system, with an average absorption of 6.53 kW.

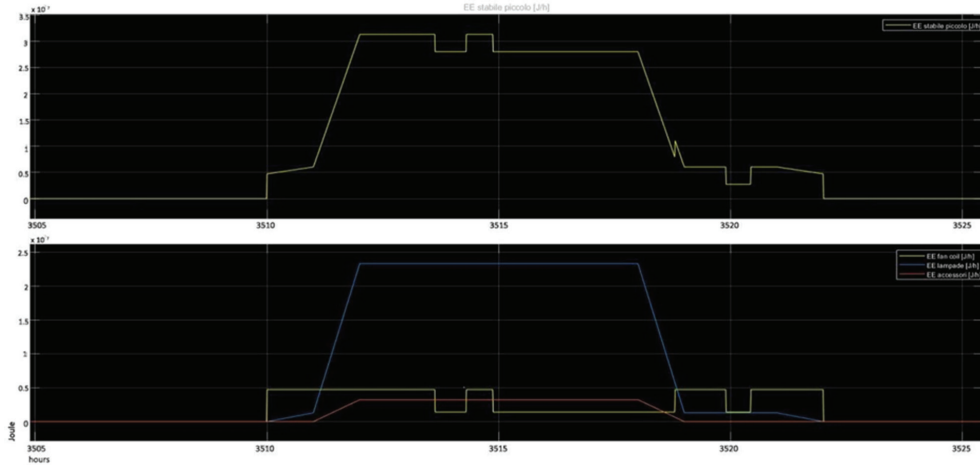


Figure 15: Building 2 daily load curve.

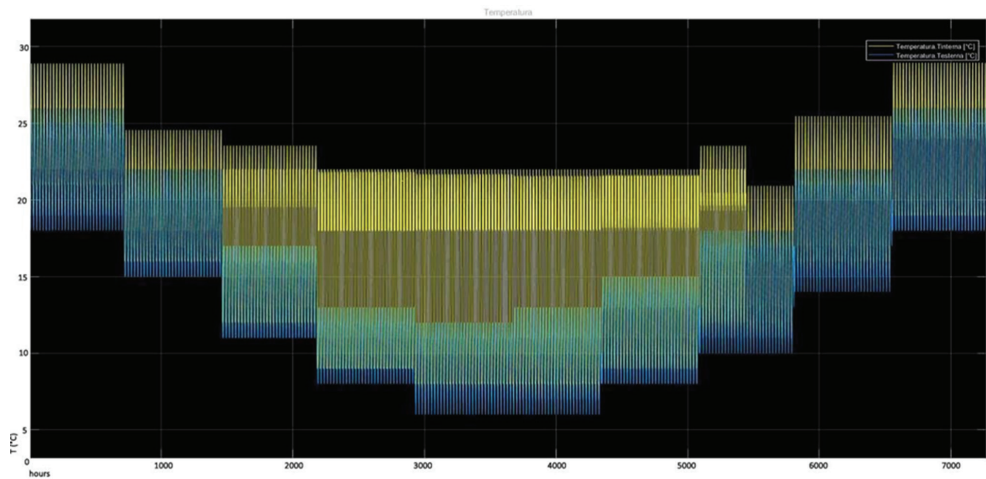


Figure 16: Building 3 global temperature trends.

4.3 Building 3

The obtained temperature results through the Building 2 simulation have the same trend as those previously reported for Building 1 (Fig. 16).

4.4 Microgrid

From the simulation carried out, it results that 346,500 kWh are needed from the national grid to feed the electrical loads of the microgrid, spending 72,760 €, considering an aver-

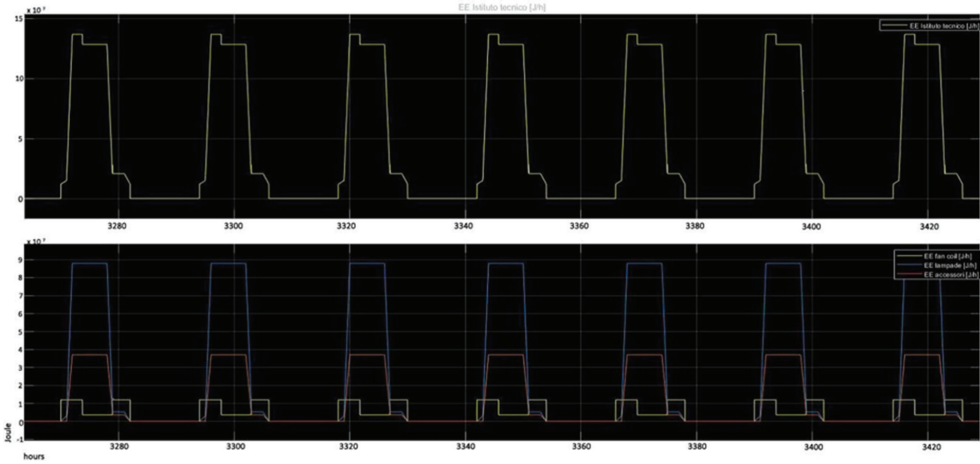


Figure 17: Building 3 weekly load curve.

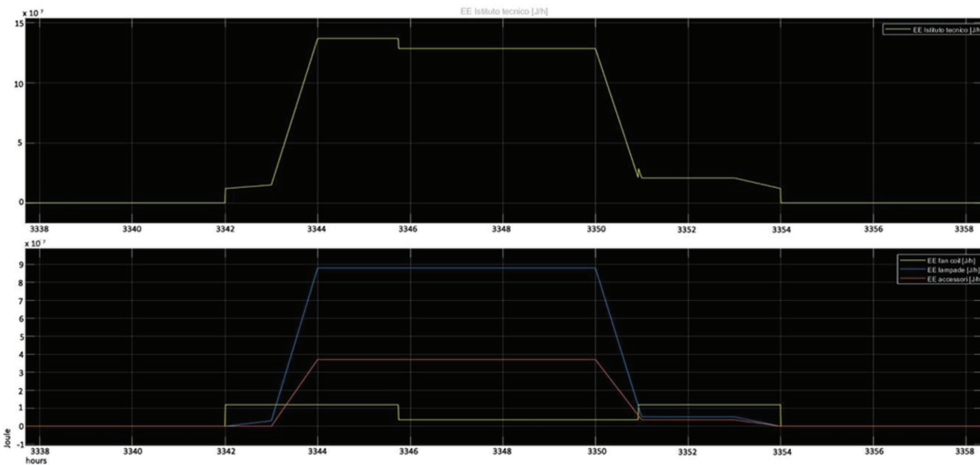


Figure 18: Building 3 daily load curve.

age price for electricity of 0.21 €/kWh. Figure 19 shows the weekly absorption for each load, while Fig. 20 shows the trend of the total electric load for 1 day, with a peak of 227.64 kW.

Figure 21 shows the hourly incident radiation on the collector plane (blue) and the net output of the photovoltaic system (yellow) with a peak of 340.55 kW.

Figure 22 shows the trend of electricity production from the PV system (blue) compared with the energy absorbed by the total electrical load (yellow). In the considered period, the percentage of consumption covered by photovoltaic generation is around 83%.

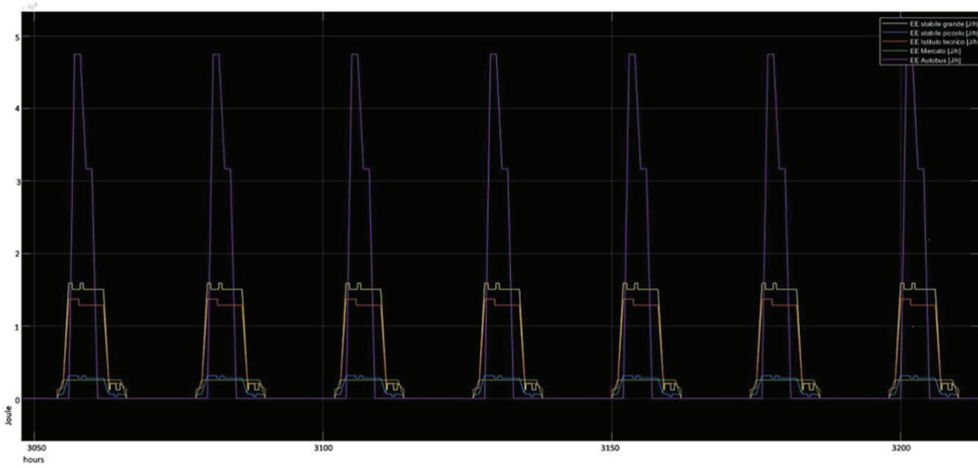


Figure 19: Weekly load curve - Total electrical loads.

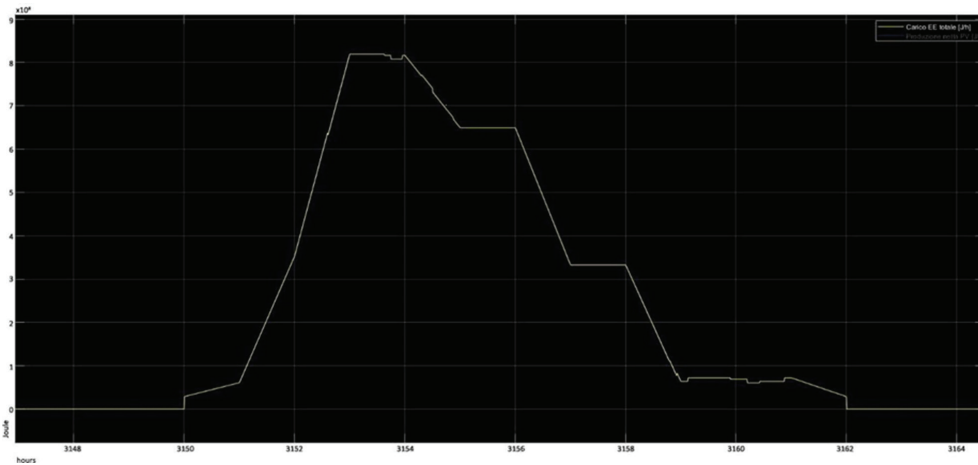


Figure 20: Daily load curve - Total electrical loads.

Moreover, from the figure, it is possible to notice that being favorable weather conditions, the production coming from the photovoltaic plant completely covers the consumption of the microgrid.

Therefore, the plant was oversized to ensure a high energy independence to the microgrid throughout the year. Especially in the warmer months, it involves an excess of electricity production available in the microgrid, with the consequent possibility to extend the system connection to a greater number of users. The total energy introduced in the microgrid amounts to 205,124.52 kWh.

Therefore, the power fed into the microgrid has the trend shown in Fig. 23.

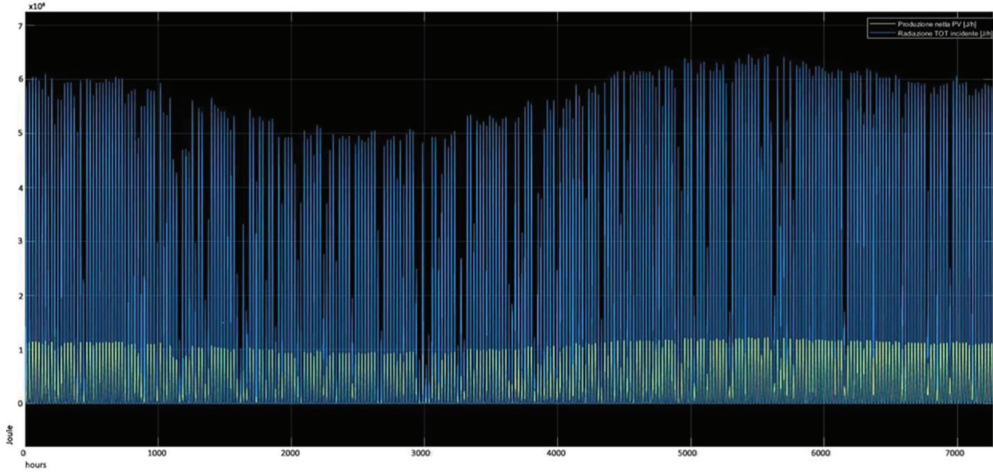


Figure 21: Hourly incident radiation vs. net PV system production.

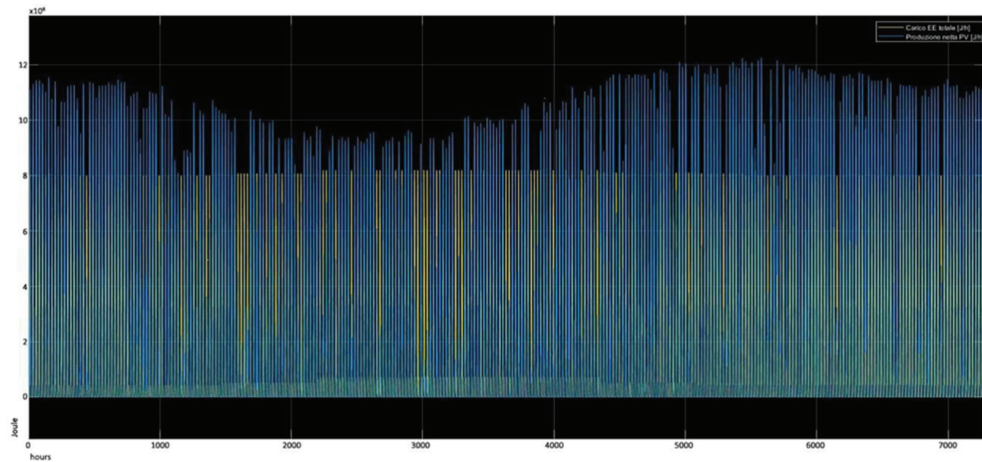


Figure 22: Total electrical loads vs. net PV system production.

From the simulation, it results that the energy not covered by the photovoltaic plant during the considered period amounts to 59,139 kWh. In case of supply lack from the network, a 250-kW EG powered by methane was set in order to ensure continuity of service, regardless of weather conditions. Also, in order to obtain a realistic simulation, it was simulated a 48-hours random failure on the net. During the system operation, the net is set to supply the energy demand. In the considered period, the energy from the net amounts to 55,216.81 kWh with a total cost of 11,595.53 €.

The power trend drawn from the grid is shown in Fig. 24, where the failure moments correspond to the sections with absorbed power equal to zero, one of which is indicated by the red arrow.

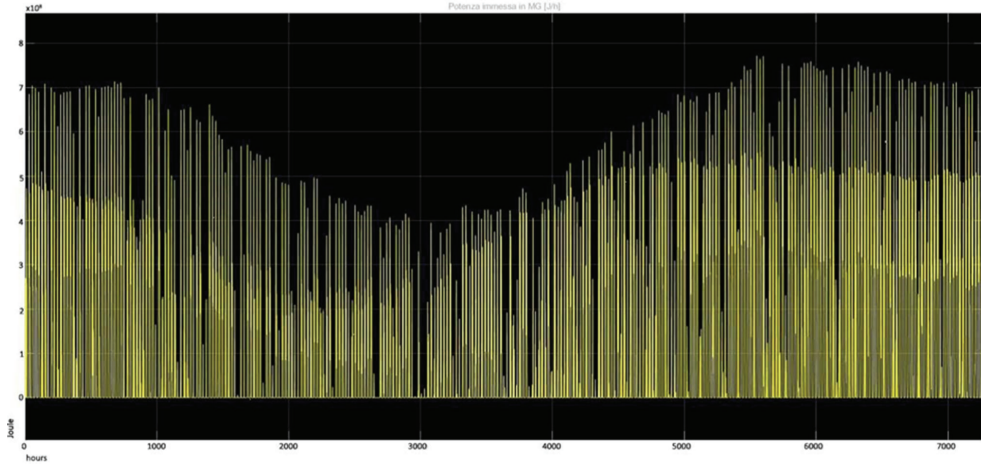


Figure 23: Trend of power fed into the microgrid.

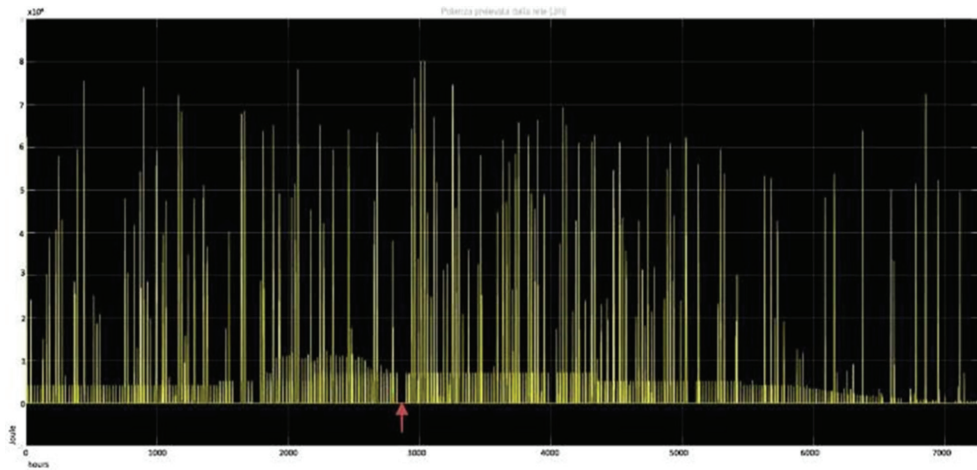


Figure 24: Trend of power drawn from the grid.

In case of failure of the national electricity grid, the EGS comes into operation, which in the considered period provides an energy equal to 3,922 kWh. The estimated methane consumption is 2,111 Sm³ with a cost of 1,161 €. Figure 25 shows the power produced by the EGS with the relative fuel consumption, supplying microgrid loads in case of power grid failure.

Thanks to the installation of the photovoltaic system and considering the cost of methane supplying the EGS, a saving on energy expenses due to the microgrid implementation is estimated to € 60,004.74 in 10 months.

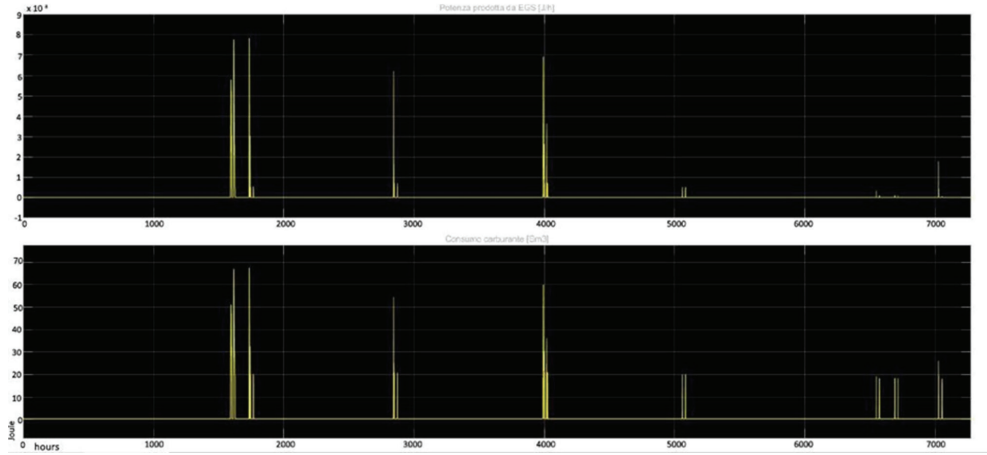


Figure 25: Trend of power produced by EGS and relative fuel consumption.

5 CONCLUSIONS

The goal of the current study was to design and simulate an electric microgrid to achieve a consistent level of community resilience, as only few research works investigated the resilience of such a system for services dedicated to public education. The microgrid system is powered by photovoltaic panels, which are not able to ensure a constant and adequate energy supply, as derived also from the literature. Therefore, the national grid will be able to cover the energy demand if the system would not be able to satisfy it.

To contrast possible blackout cases of the national network, a 250-kW EG powered by methane is integrated in the system. The results show that the microgrid consumption is completely covered by the electricity production from the photovoltaic system during the summer period. In fact, the plant is oversized in order to ensure a high energy independence to the microgrid throughout the year. Especially in the warmer months, it involves an excess in the electricity production by the microgrid, useful in case of extending the system to a greater number of users. The share of energy required by the national grid corresponds to 59,139 kWh. In case of a blackout, the activation of the diesel generator guarantees a coverage of the service, as demonstrated through the 48-hour simulated blackout. In summary, the proposed microgrid system and EG allow an overall saving on energy expenses for power supply of the school buildings of € 60,004.74 in 10 months.

The use of an intelligent energy demand monitoring system for the microgrid will be developed in future research.

REFERENCES

- [1] Hirscha, A., Paraga, Y. & Guerrerob, J., Microgrids: A review of technologies, key drivers, and outstanding issues. *Renewable and Sustainable Energy Reviews*, **90**, pp 402–411, 2018. <https://doi.org/10.1016/j.rser.2018.03.040>
- [2] DIRECTIVE (EU) 2018/2001 OF THE EUROPEAN PARLIAMENT AND OF THE COUNCIL of 11 December 2018 on promoting the use of energy from renewable sources (recast).

- [3] Williams, N. J., Jaramillo, P., Taneja, J. & Ustun, T. S., Enabling private sector investment in microgrid-based rural electrification in developing countries: a review. *Renew Sustain Energy Rev*, **52**, pp. 1268–1281, 2015. <http://dx.doi.org/10.1016/j.rser.2015.07.153>
- [4] Akorede, M. F., Hizam, H. & Pouresmaeil, E., Distributed energy resources and benefits to the environment. *Renew Sustain Energy Rev*, **14**, pp. 724–734, 2010. <http://dx.doi.org/10.1016/j.rser.2009.10.025>
- [5] Bayindir, R., Hossain, E., Kabalci, E. & Perez, R., A comprehensive study on microgrid technology. *Int J Renew Energy Res.* **4**, pp. 1094–1107, 2014.
- [6] Mekhilef, S., Saidur, R. & Safari, A., Comparative study of different fuel cell technologies. *Renew Sustain Energy Rev*, **16**, pp. 981–989, 2012.
- [7] Abusharkh, S., Arnold, R., Kohler, J., Li, R., Markvart, T., Ross, J., et al. Can microgrids make a major contribution to UK energy supply? *Renew Sustain Energy Rev*, **10**, pp. 78–127, 2006.
- [8] Elder, B., Docket No. 39732 e notice of inquiry and workshop to examine issues related to the value of renewable and distributed energy resources in preparations for the 2016 Georgia power company integrated resource plan (IRP). Cary: Keyes, Fox and Wiedman LLP; 2015.
- [9] Thornton, A. & Rodríguez-Monroy, C., Distributed power generation in the United States. *Renew Sustain Energy Rev*, **15**, pp. 4809–4817, 2011. <https://doi.org/10.1016/j.rser.2011.07.070>
- [10] Mattoni, B., Pompei, L., Losilla, J. C. & Bisegna, F., Planning smart cities: Comparison of two quantitative\multicriteria methods applied to real case studies. *Sustainable Cities and Society*, **60**, 2020.
- [11] Leskarac, D., Moghimi, M., Liu, J., Water, W., Lu, J., Stegen, S., et al. Hybrid AC/DC Microgrid testing facility for energy management in commercial buildings. *Energy Build*, **174**, pp. 563–78, 2018. <https://doi.org/10.1016/j.enbuild.2018.06.061>
- [12] Kampelis, N., Gobakis, K., Vagias, V., Kolokotsa, D., Standardi, I., Isidori, D., et al. Evaluation of the performance gap in industrial, residential & tertiary near-Zero energy buildings. *Energy Build*, **148**, pp. 58–73, 2017. <https://doi.org/10.1016/j.enbuild.2017.03.057>
- [13] Gonzalez-Mahecha, R. E., Lucena, A. F. P., Szklo, A., Ferreira, P., Vaz, A. I. F. Optimization model for evaluating on-site renewable technologies with storage in zero/nearly zero energy buildings. *Energy Build*, **172**, pp. 505–516, 2018. <https://doi.org/10.1016/j.enbuild.2018.04.027>
- [14] Sechilariu, M., Wang, B. & Locment, F. Building-integrated microgrid: advanced local energy management for forthcoming smart power grid communication. *Energy Build*. **59**, pp. 236–243, 2013. <https://doi.org/10.1016/j.enbuild.2012.12.039>
- [15] Rosales-Asensio, E., de Simón-Martín, M., Borge-Diez, D., Blanes-Peiró, J. J., Colmenar-Santos, A. Microgrids with energy storage systems as a means to increase power resilience: An application to office buildings. *Energy*, **172**, pp. 1005–1015, 2019. <https://doi.org/10.1016/j.energy.2019.02.043>
- [16] EN 12464-1:2011. Light and lighting - Lighting of work places - Part 1: Indoor work places.
- [17] Decreto ministeriale (Ministero dei lavori pubblici) 18-12-1975. Norme tecniche aggiornate relative all'edilizia scolastica, ivi compresi gli indici di funzionalità didattica, edilizia ed urbanistica, da osservarsi nella esecuzione di opere di edilizia scolastica.
- [18] PVSYSYST Photovoltaic Software, <https://www.pvsyst.com/software-evaluation> [Accessed: 8- February-2021].